Journal of Alloys and Compounds 504S (2010) S186–S189

Contents lists available at ScienceDirect

Journal of Alloys and Compounds

journal homepage: www.elsevier.com/locate/jallcom

Quasicrystal-like structure and its crystalline approximant in an $Fe_{48}Cr_{15}Mo_{14}C_{15}B_6Tm_2$ bulk metallic glass

Akihiko Hirata[a,*], Yoshihiko Hirotsu[b], Kenji Amiya[c], Akihisa Inoue[a]

[a] WPI Advanced Institute for Materials Research, Tohoku University, 2-1-1 Katahira, Sendai 980-8577, Miyagi, Japan
[b] R&D Institute of Metals and Composites for Future Industries (RIMCOF), Osaka University Laboratory, Osaka 567-0047, Japan
[c] Institute for Materials Research, Tohoku University, Sendai 980-8577, Japan

ARTICLE INFO

Article history:
Received 1 July 2009
Received in revised form 23 March 2010
Accepted 31 March 2010
Available online 8 April 2010

Keywords:
Bulk metallic glass
Crystallization
Nanobeam electron diffraction
Quasicrystal

ABSTRACT

Nanoscale quasicrystal-like structural states have been found in the course of crystallization in an Fe-based $Fe_{48}Cr_{15}Mo_{14}C_{15}B_6Tm_2$ bulk metallic glass. The quasicrystal-like structure is similar with the χ-FeCrMo structure exhibiting a deformed tenfold diffraction pattern due to projected pentagonal arrangements regarded as a Mo framework. We show the preliminary structural model for the quasicrystal-like structure and discuss the three-dimensional features based on the χ-FeCrMo crystalline approximant.

1. Introduction

Local structural similarity between glass and crystal (or quasicrystal) structures has been extensively discussed in the field of metallic glasses. For Zr-based metallic glasses, it is widely accepted that icosahedral atomic arrangements are one of the dominant structural units [1–5] and their fraction gets an increase with improving the glass forming ability [6,7]. During the crystallization processes, additionally, many researchers have reported that icosahedral quasicrystals or complex crystal structures (e.g. Ti_2Ni-type) comprising icosahedral atomic arrangements are directly formed from the glass states [1,8–13]. Considering these facts, it is likely that there is a structural linkage among the glass, quasicrystal, and crystal states with respect to the icosahedral atomic configurations in Zr-based metallic glasses [1,2]. Crystal states, which can be regarded as crystalline approximants [14] for quasicrystals, are especially important, because atomic configurations in crystals can be determined without uncertainty. It is therefore necessary to observe the structural relationship of all the three states in continuous structural developments.

Recently, we have examined a crystallization process of an $Fe_{48}Cr_{15}Mo_{14}C_{15}B_6Tm_2$ bulk metallic glass (BMG) [15] which exhibits a quite high glass stability [16]. During the crystallization, we found a χ-FeCrMo (α-Mn type) structure corresponding to the first peak of the double exothermic DSC peaks. In previous works, the α-Mn type structure was frequently found in Fe-based metallic glasses [17–22]. Before the formation of χ-FeCrMo, moreover, χ-FeCrMo-like structures similar to quasicrystals were also observed as nanograins with a size of about 5 nm [23]. From such nanoscale regions, we have successfully obtained pseudo tenfold electron diffraction patterns like a quasicrystal using a TV-recording nanobeam electron diffraction (NBED) method. The χ-FeCrMo structure was judged to be a crystalline approximant of the quasicrystal-like structure based on an existence of the intermediate state. By using structural motifs of χ-FeCrMo, we have proposed a preliminary projected (two-dimensional) structural model for the quasicrystal-like structure [23]. In this paper, we discuss the three-dimensional structural features of the quasicrystal-like structure based on the χ-FeCrMo crystalline approximant.

2. Experimental procedure

A ribbon of $Fe_{48}Cr_{15}Mo_{14}C_{15}B_6Tm_2$ metallic glasses was made by using the single-roll rapid quenching technique. The ribbon specimens were annealed isothermally at 873, 923, and 973 K for 0.5 h in a vacuum furnace. Specimens for TEM observation were prepared by electropolishing (acetic-perchloric acid) at room temperature followed by Ar ion-milling. NBED patterns were taken using a JEM-3000F TEM (300 kV) and recorded from place to place using a TV-rate video camera by scanning a nanoprobe (diameter: ~1 nm) at a speed of ~10 nm/s. More than 50,000 frames were recorded on the video tape and symmetric patterns were selected for analyzing local structures. The amount of electron dose for the nanoprobe in NBED was about 2.0×10^{19} e/cm^2 measured by a Faraday gauge, which is almost 10 times smaller than that for the conventional HREM imaging.

* Corresponding author.
E-mail address: hirata@wpi-aimr.tohoku.ac.jp (A. Hirata).

0925-8388/$ – see front matter © 2010 Elsevier B.V. All rights reserved.
doi:10.1016/j.jallcom.2010.03.222

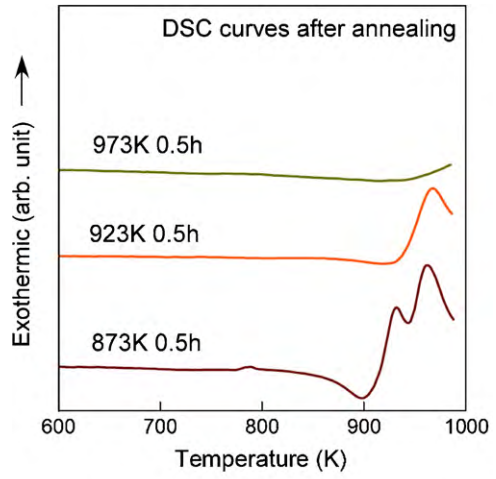

Fig. 1. DSC curves obtained from the specimen isothermally annealed at 873, 923, and 973 K for 0.5 h.

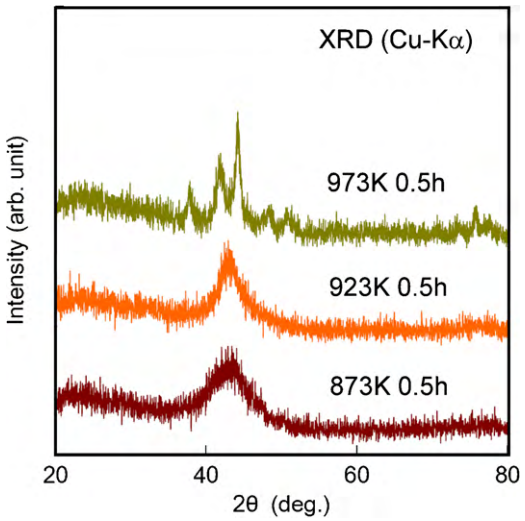

Fig. 2. X-ray diffraction profiles obtained from the specimen isothermally annealed at 873, 923, and 973 K for 0.5 h.

3. Results and discussion

Fig. 1 shows differential scanning calorimeter (DSC) curves obtained from the specimens after being annealed at 873, 923, and 973 K for 0.5 h. The measurements for each specimen were performed with a heating rate of 40 K/min. The DSC curve for the specimen annealed at 873 K shows double exothermic peaks around 950 K. The first exothermic peak disappeared after annealing at 923 K, and the second peak also disappeared after annealing at 973 K. These facts indicate that the first and second reactions completed after annealing at 923 and 973 K, respectively. Fig. 2 shows X-ray diffraction profiles (Cu-Kα) obtained from the specimens annealed at 873, 923, and 973 K for 0.5 h. Distinct diffraction peaks from crystals can be seen only in the profile of the specimen annealed at 973 K (after the second exothermic peak in DSC). Below 923 K, it is difficult to observe diffraction peaks in the profiles, although the first halo intensity gradually increases. Therefore, it is necessary to get fine scale structural information using a NBED technique in a transmission electron microscope.

A characteristic NBED pattern with pseudotenfold symmetry obtained from the specimen annealed at 923 K is shown in Fig. 3(a). We can see pseudotenfold diffraction patterns with ten strong diffraction spots along the first and second halo rings in the pattern. Although the NBED pattern is almost tenfold, distances between neighboring diffraction spots observed on the first halo ring were found to be fluctuated within 10%. Fig. 3(b) shows an [1 1 3] zone-axis pattern of the χ-FeCrMo structure obtained from the identical specimen. In the pattern of (b), we see a deformed tenfold pattern consisting of diffraction spots arranged with a periodicity. It is important that the spots with relatively strong intensities make up the deformed tenfold pattern. The complicated intensity distribution is considered to come from a structural complexity of the χ-FeCrMo structure. We also found the intermediate state between the quasicrystal-like and χ-FeCrMo structures. On the basis of this fact, the χ-FeCrMo structure can be regarded as a crystalline approximant of the quasicrystal-like structure.

We tried to construct a preliminary structural model of the quasicrystal-like structure based on the χ-FeCrMo crystalline approximant. Fig. 4(a) shows the [1 1 3] projection of the χ-FeCrMo structure with respect to a Mo framework. All the atoms projected on (1 1 3) including Fe and Cr atoms are depicted in the upper left part. A linkage of pentagons constructed by Mo atoms can be seen

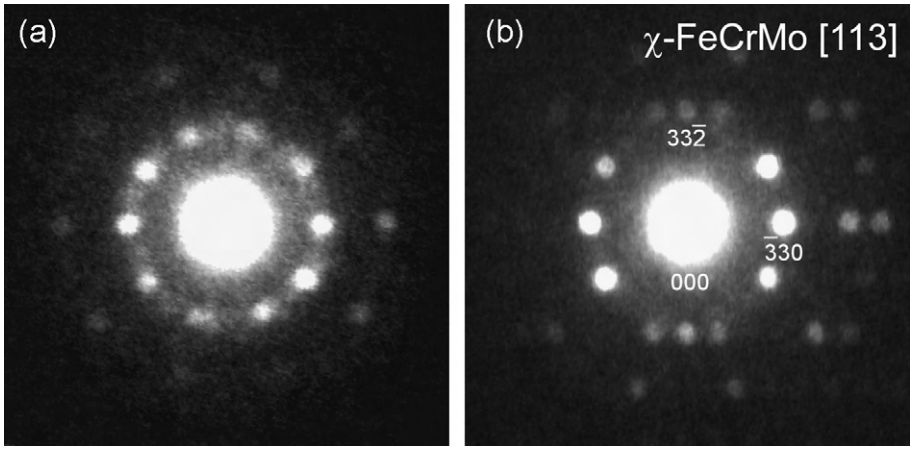

Fig. 3. (a) Pseudo tenfold NBED pattern and (b) [1 1 3] zone-axis NBED pattern of the χ-FeCrMo structure obtained from the specimen annealed at 923 K for 0.5 h.

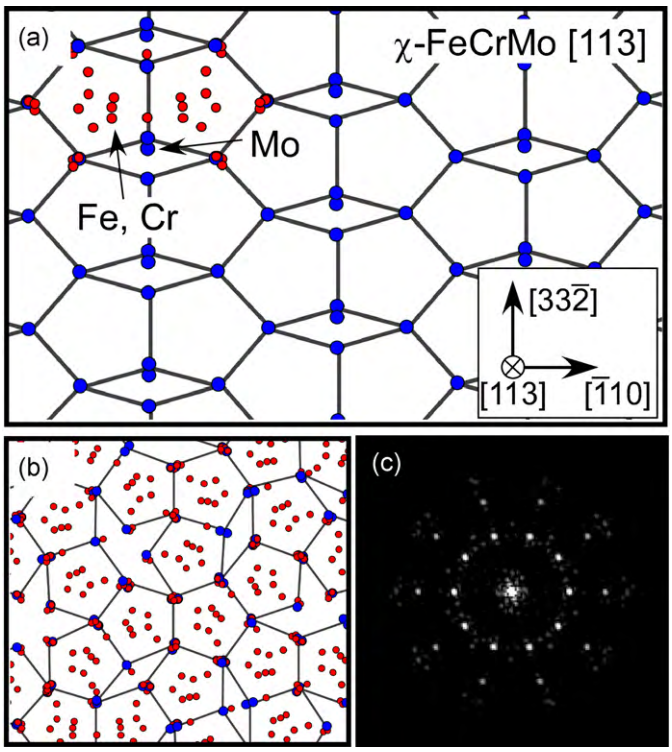

Fig. 4. (a) [1 1 3] projection of the χ-FeCrMo structure with respect to the Mo linkage in which the pentagonal tiles are arranged regularly. All the atoms including Fe and Cr are shown at the upper left. (b) Preliminary structure model of the quasicrystal-like structure and (c) Fourier transform pattern obtained from the model.

in a periodic manner. We made a projected structural model of the quasicrystal-like structure using the pentagons as structural motifs as shown in Fig. 4(b). The pentagonal structural motifs are linked by shearing their edges to fill the two-dimensional space. A Fourier transform spectrum obtained from the model shown in Fig. 4(c) is well consistent with the experimental NBED pattern (Fig. 3(a)). Note that this is just a projected structure model, not a three-dimensional model. If there is a quasi-periodicity along the projected direction ([1 1 3] direction), we cannot know the exact atomic arrangement in analogy with icosahedral quasicrystals. However, it is important to try to understand the three-dimensional structural features of the structural motifs found in the χ-FeCrMo structure.

Fig. 5 shows atomic configurations of a single structural motif consisting of two projected pentagons formed by Mo atoms. The [1 1 3] and [3 3 $\bar{2}$] projections of the χ-FeCrMo structure are depicted in Fig. 5(a) and (b), respectively. The larger circles denote Mo atoms and smaller ones Fe or Cr atoms. In the [1 1 3] projection of (a), it appears that the two pentagons are formed by the Mo atoms. However, each Mo atom is not positioned in the same (1 1 3) plane as shown in Fig. 5(b). Accordingly, it can be said that we just see apparent pentagons formed by Mo atoms in the [1 1 3] projection. In the [3 3 $\bar{2}$] projection of (b), a distance between the upper side and the lower side Mo atoms denoted by 4 or 7 is about 1.49 nm, which corresponds to the one period along the [1 1 3] direction. As shown in figure, the period can be divided into five sections with respect to the Mo layers, where a ratio a:b:c:d:e of the distances between each layer is just equal to 6:3:3:4:6. Note that only the Mo atom denoted by 1 is slightly deviated from the Mo layer defined by the ratio of integers. Although the χ-FeCrMo structure is considerably complex, the quasicrystal-like structure should be much more complicated. In addition, the grain size is quite small (~5 nm) and the structure is less ordered in comparison with stable quasicrystals (e.g. Al-based alloys [24]). These factors make it more difficult to reveal an atomic configuration of the quasicrystal-like structure.

Here we consider how the structural motifs are connected each other in the structural model of the quasicrystal-like structure. Although it is very difficult to solve the three-dimensional structure, it is worth considering a rough picture for this complex structure. Fig. 6 shows four possible connections of the structural motifs found in our preliminary model (Fig. 4(b)). In each figure, two structural motifs are connected each other by sharing their edges. A number of each Mo atom, which is identical to that in Fig. 5, is shown in the pictures. These atoms are found to take part in the connection between two structural motifs. A connection manner of (a) is just the same as that of the χ-FeCrMo structure. The atoms 2 and 3 can be connected with atoms 8 and 7 by a shift of 0.41 nm (=1.49 × 6/(6 + 3 + 3 + 4 + 6)) along the direction perpendicular to the sheet (tenfold axis). In a case of (b), a shift of 0.68 nm (=1.49 × (3 + 3 + 4)/(6 + 3 + 3 + 4 + 6)) is needed for the connection. No shift is necessary for a case of (c). As for a case of (d), a shift of 0.68 nm (=1.49 × (4 + 6)/(6 + 3 + 3 + 4 + 6)) leads to connect the pentagons, if we exclude the atom denoted by 1 at the special position from consideration. In all the cases, as shown above, the local structural matchings are basically well even allowing for the three-dimensional atomic configurations.

4. Conclusions

The quasicrystal-like structure similar to the χ-FeCrMo structure was found in the course of the crystallization in an $Fe_{48}Cr_{15}Mo_{14}C_{15}B_6Tm_2$ bulk metallic glass. We have discussed the three-dimensional structural features of the quasicrystal-like structure based on the χ-FeCrMo structure which can be regarded as a crystalline approximant. Although it is difficult to solve the three-dimensional atomic configuration of the quasicrystal-like

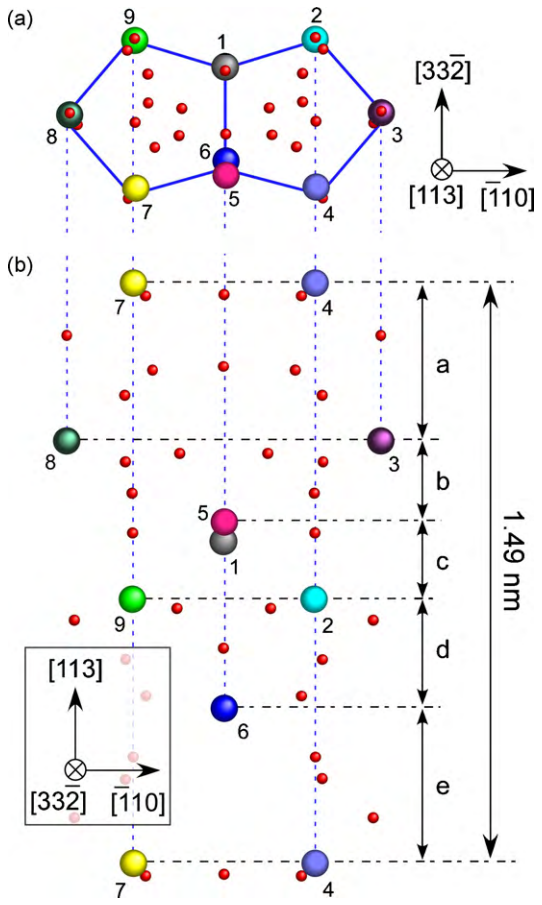

Fig. 5. (a) [1 1 3] and (b) [3 3 $\bar{2}$] projections of a single structural motif found in the χ-FeCrMo structure. The structural motifs are used in the structure model of the quasicrystal-like structure shown in Fig. 4. Larger circles denote Mo atoms, which are numbered, and smaller circles Fe or Cr atoms.

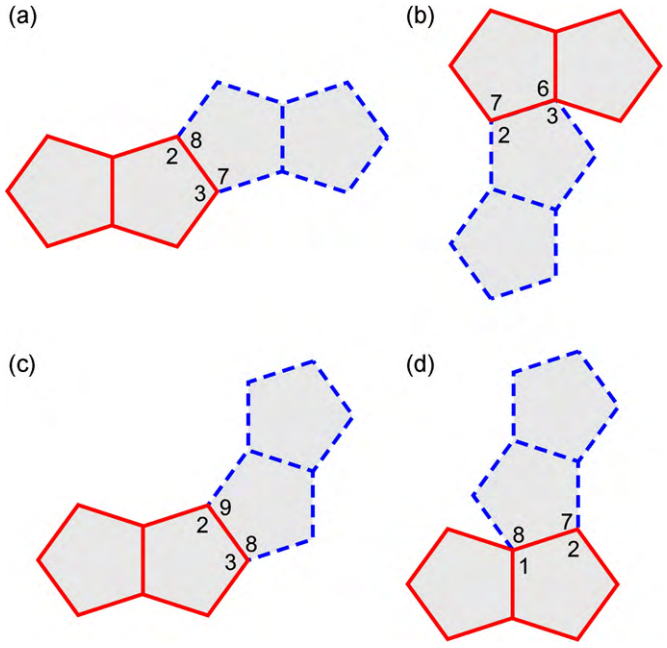

Fig. 6. Four types of possible connection manners of the structural motifs. These connection manners can be found in our preliminary model shown in Fig. 4. The number for each atom is identical to that used in Fig. 5.

structure, we tried to provide a rough picture with respect to a Mo framework. The Mo atoms forming pentagons found in the projected model of the quasicrystal-like structure are not positioned in the same plane three-dimensionally. Structural matchings between the structural motifs in some possible cases are well even in the three-dimensional structure model.

Acknowledgment

A. H. acknowledges support from the Ministry of Education, Culture, Sports, Science and Technology, Japan (Grant-in-Aid for Young Scientists No. 20760442). A. H. would also like to sincerely thank A. Koreeda for his technical assistance.

References

[1] K.F. Kelton, G.W. Lee, A.K. Gangopadhyay, R.W. Hyers, T.J. Rathz, J.R. Rogers, M.B. Robinson, D.S. Robinson, Phys. Rev. Lett. 90 (2003) 195504.
[2] C. Dong, Q. Wang, J.B. Qiang, Y.M. Wang, N. Jiang, G. Han, Y.H. Li, J. Wu, J.H. Xia, J. Phys. D: Appl. Phys. 40 (2007) R273.
[3] H.W. Sheng, W.K. Luo, F.M. Alamgir, J.M. Bai, E. Ma, Nature (London) 439 (2006) 419.
[4] T. Takagi, T. Ohkubo, Y. Hirotsu, B.S. Murty, K. Hono, D. Shindo, Appl. Phys. Lett. 79 (2001) 485.
[5] A. Hirata, T. Morino, Y. Hirotsu, K. Itoh, T. Fukunaga, Mater. Trans. 48 (2007) 1299.
[6] T. Fukunaga, K. Itoh, T. Otomo, K. Mori, M. Sugiyama, H. Kato, M. Hasegawa, A. Hirata, Y. Hirotsu, A.C. Hannon, Mater. Trans. 48 (2007) 1698.
[7] Y.Q. Cheng, E. Ma, H.W. Sheng, Phys. Rev. Lett. 102 (2009) 245501.
[8] U. Köster, J. Meinhardt, S. Roos, H. Liebertz, Appl. Phys. Lett. 69 (1996) 179.
[9] C. Li, A. Inoue, Phys. Rev. B 63 (2001) 172201.
[10] J. Saida, A. Inoue, J. Non-Cryst. Solids 317 (2003) 97–105.
[11] T. Waniuk, J. Schroers, W.L. Johnson, Phys. Rev. B 67 (2003) 184203.
[12] I. Martin, T. Ohkubo, M. Ohnuma, B. Deconihout, K. Hono, Acta Mater. 52 (2004) 4427.
[13] K. Kajiwara, M. Ohnuma, T. Ohkubo, D.H. Ping, K. Hono, Mater. Sci. Eng. A 738 (2004) 375–377.
[14] V. Elser, C.L. Henley, Phys. Rev. Lett. 55 (1985) 2883.
[15] K. Amiya, A. Inoue, Mater. Trans. 47 (2006) 1615.
[16] A. Hirata, Y. Hirotsu, K. Amiya, A. Inoue, Phys. Rev. B 78 (2008) 144205.
[17] A. Inoue, T. Iwadachi, T. Minemura, T. Masumoto, Mater. Trans. JIM 22 (1981) 197.
[18] V.C. Chen, C.M. Chen, K. Su, Mater. Sci. Eng. A133 (1991) 596.
[19] M. Ohnuma, O. Sasaki, H. Kuwano, S. Katano, Y. Morii, S. Funahashi, H.R. Child, Y. Hamaguchi, Mater. Trans. JIM 34 (1993) 874.
[20] M. Imafuku, S. Sato, H. Koshiba, E. Matsubara, A. Inoue, Scripta Mater. 44 (2001) 2369.
[21] I.V. Lyasotskii, N.B. Dyakonova, E.N. Vlasova, D.L. Dyakonov, M.Yu. Yazvitskii, Phys. Stat. Sol. (a) 203 (2006) 259.
[22] N.B. Dyakonova, I.V. Lyasotskii, E.N. Vlasova, D.L. Dyakonov, B.V. Molotilov, Adv. Perform. Mater. 4 (1997) 199.
[23] A. Hirata, Y. Hirotsu, K. Amiya, A. Inoue, Phys. Rev. B 79 (2009) 020205R.
[24] K. Hiraga, A. Bo-Ping Zhang, T. Inoue, Masumoto, Jpn. J. Appl. Phys. 27 (1988) L951.